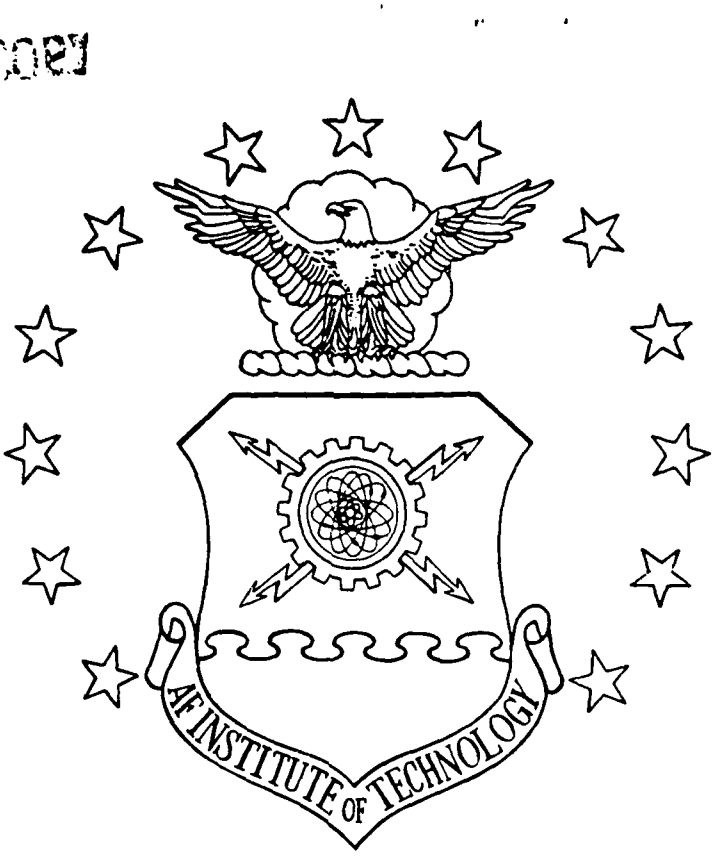

COMPARISON OF BASIS FUNCTION AND ITERATION SOLUTIONS TO THE FREDHOLM INTEGRAL EQUATION OF THE FIRST KIND

THESIS

Michael E. Carter
Captain, USAF

AFIT/GNE/ENP/89M-1

DEPARTMENT OF THE AIR FORCE
AIR UNIVERSITY
AIR FORCE INSTITUTE OF TECHNOLOGY

Wright-Patterson Air Force Base, Ohio

AFIT/GNE/ENP/89M-1

COMPARISON OF BASIS FUNCTION AND ITERATION SOLUTIONS TO THE FREDHOLM INTEGRAL EQUATION OF THE FIRST KIND

THESIS

Michael E. Carter
Captain, USAF

AFIT/GNE/ENP/89M-1

AFIT/GNE/ENP/89M-1

COMPARISON OF BASIS FUNCTION AND ITERATION SOLUTIONS TO THE FREDHOLM INTEGRAL EQUATION OF THE FIRST KIND

THESIS

Presented to the Facility of the School of Engineering

of the Air Force Institute of Technology

Air University

In Partial Fulfillment of the

Requirements for the Degree of

Master of Science in Nuclear Engineering (Effects)

Michael E. Carter, B.S.

Captain, USAF

March 1989

Preface

The purpose of this study is to compare the basis function and iteration methods for solving the Fredholm integral equations of the first kind. The equation arises in the analysis of data from underground nuclear effects simulations. The Fredholm equation is ill-posed and so its answer is dependent upon the method of solution.

Often the Fredhom equation is solved with the iteration method tested here, but the basis function method, tested by Capt Russell Daniel, is another productive approach.

There are two people that I would like to thank for their help during this study. First I am indebted to my faculty advisor, LCDR Kirk A. Mathews, for his help and patience during this study. The second person is Capt Russell Daniel. His program and thesis were essential to my understanding of the basis function method.

Michael E. Carter

Table of Contents

Table of Figures

Abstract

The purpose of this study is to compare methods for solving the Fredholm integral equation of the first kind. The Fredholm equation has several practical applications including geology, superconductivity, and aerodynamics. Of specific interest is its application to determining radiation spectra using data from underground nuclear effects simulations.

The two basic solution methods studied were the basis function and the iteration methods. The basis function method is a representation of the unfolded spectrum by a series of Planckian or cubic spline functions. The iteration method scales the unfolded spectrum so that its weighted integral over a given interval matches that of the actual spectrum.

Both basis function methods produced excellent results when the actual spectrum was a sum of it's basis functions. The cubic spline method produced unfolded spectra which were good approximations for discontinuous actual spectra. However, there was a significant dropoff of the spectrum for the cubic spline for higher energies.

The iteration method produced accurate approximations for actual spectra that were both basis function and discontinuous spectra. There were two problems with this method: the unfolded spectra were discontinuous at the discontinuities of the weighting function and noisy data sometimes produced large discontinuities in the unfolded spectra.

For the four test cases studied, the iteration method proved to be the best because of it's ability to unfold a variety of spectra (in contrast to the Planckian basis function method) and it's good behavior at higher energies for noisy data (in contrast to the cubic spline method).

I. Introduction

Background

The Fredholm integral equation of the first kind has widespread application in areas such as acoustics, optics (3:1-1), superconductivity, geophysics, and aerodynamics (4:261-263). A particular application of the Fredholm equation is to determine the radiation spectra of simulated nuclear weapons effects. The terminology in this study originates from this application.

The Fredholm integral equation of the first kind has the following form:

$$Y(\epsilon) = \int_a^b R(\epsilon, \eta) s(\eta) d\eta \qquad (1)$$

where

$Y(\epsilon)$ = detector output signal

$R(\epsilon, \eta)$ = detector response function

$s(\eta)d\eta$ = radiation spectrum

In this application, the practical aspects of data collection force several limitations on the detectors. The limitations occur because the number of detectors is finite, the detectors have a finite resolution, $E/\Delta E$, and recording, transmitting, and calibrating errors affect the data.

Recording and transmitting errors are reduced by using two types of detectors, "open" (fluorescer system) and "closed" (filter/fluorescer system) response detectors. Theoretical modeling and calibration measurements determine the response functions of the detectors.

Problem

The Fredholm equation is ill-posed; therefore, there are an infinite number of spectra, $s(\eta)d\eta$ which would have the same detector output, $Y(\epsilon)$ The three methods of unfolding used in this study each produce an approximate solution to the Fredholm equation. The main purpose of this study is to compare how well the approximate spectra, from these methods, reproduce the original spectrum. To do this comparison, all three methods of solution were incorporated into a computer program.

Scope

Three approximate methods for solving Equation (1) will be used during this study: the basis function method, the iteration method, and the modified iteration method.

The measured signals were calculated assuming the actual spectrum, which in practice would not be known. The unfolding methods produce unfolded spectra. These unfolded spectra are then compared to the actual spectrum.

There are four actual spectra that will be used in this study to compare these methods: a two-temperature Planckian spectrum with a spike

added for reasonable detail, a Heaviside function, a spike on a flat spectrum, and a triangular spike on a flat spectrum.

The first spectrum represents a simplified version of expected nuclear effects radiation; the basic spectrum being composed of multiple Planckians with the spike added as a reasonable detail. The latter three spectra are tested to see how the unfolding methods deal with different discontinuous behavior.

The tests were conducted first on unfolded spectra with no noise. This indicates how well the methods intrinsically work. Then the methods were applied to the same spectra in a more realistic environment of experimental uncertainties.

Assumptions

In order to compare with previous work by Daniel (3) similar assumptions are made. They are:

1. There are 20 detectors. 13 of these are "closed" and 7 are "open" response detectors.
2. The resolving power of the detectors, $E/\Delta E$, is approximately 1.5.
3. The response functions are exact. Their exact form is given in Section II.

Also, several tacit assumptions are made to restrict the infinite number of solutions to the unique unfolded spectrum given by the methods studied. These depend upon the method used and are discussed in Section II.

General Approach

The actual spectrum, which is in practice unknown, is assumed in order to calculate the measured signal by an approximate solution of Equation (1). One of the three unfolding methods is then used to determine the unfolded spectrum, given the measured signal and the detector response function.

For the basis-function method, a χ^2 test statistic is used to stop the method. The iteration methods are, in practice, stopped when the spectrum is judged reasonable. If the method is stopped too soon, the effects of the smoother have not yet had a chance to work. If the method is stopped too late, all the details of the spectrum have been washed out.

The unfolded spectra will then be compared to the original spectrum, the actual spectrum, and the spectra of the other methods.

Sequence of Presentation

The presentation of the rest of the study is as follows. Chapter II, "Theoretical Discussion", details the theory of the unfolding techniques used. Chapter III, "Computer Program Implementation", describes the program which implements the unfolding techniques. Chapter IV, "Results and

Discussion", reviews the results of the unfolding techniques. Chapter V, "Conclusion and Summary", summarizes the results and presents the conclusions.

II. Theoretical Development

Introduction

In this chapter the theoretical background of several unfolding techniques are discussed. The following topics are addressed: the detector response function, the definition of the spectra, the definition of the signals, the definition of unfolding methods, the flux non-negativity constraint, the formulation of the χ^2 test statistic, the minimization of the χ^2 statistic, and the normal distribution for simulating measurement error.

Linear Fredholm Integral Equation of the First Kind

The detectors, used to measure spectra of underground nuclear simulations, are designed to have an output proportional to the spectrum in the energy range E to $E + \Delta E$

$$y_i(E)\Delta E = R_i(E)s(E)\Delta E \qquad (2)$$

where

$y_i(E)\Delta E$ = is the incremental output of detector i due to the spectrum in the energy range E to $E + \Delta E$

$R_i(E)$ = response of detector i to the part of the spectrum at the energy E

$s(E)\Delta E$ = the amount of the spectrum that is in the energy range E to $E + \Delta E$

The output signal of detector i due to the total spectrum would be:

$$Y_i = \int_0^{\infty} y_i(E)dE = \int_0^{\infty} R_i(E)s(E)dE \qquad (3)$$

where

Y_i = the output signal of detector i in response to the entire energy spectrum.

This is a linear Fredholm integral equation of the first kind.

Detector Response Function

The detector response function, $R_i(E)$, is the normalized output of detector, i, due to the portion of the spectrum at the energy E. These response functions are calibrated to a known spectrum and are assumed for this study to be the same for the unknown source being measured.

In a realistic experiment, multiple detectors (response functions) are used simultaneously and their results are compared in an effort to reduce measurement errors. There are two types of response functions used in this study: "open" and "closed". The "open" detector system is a fluorescer detector that has a zero response for energies less than the k-edge of the fluorescer and an exponentially-decreasing response for higher energies as shown in Figure I.

The equation for the "open" response function (3:3-3) is given by:

$$R_i^{open}(E) = \begin{cases} 0 & for \quad E < E_i^0 \\ \left(\frac{1}{E}\right)\left\{1 - \exp\left[-3\left(\frac{E_i^0}{E}\right)^3\right]\right\} & for \quad E \geq E_i^0 \end{cases} \tag{4}$$

where

$R_i^{open}(E)$ = the response function for the "open" detector i

E_i^0 = the k-edge of the fluorescer for detector i

E = energy

Figure I is an example of an "open" response function. The sensitivity is the amplitude of the response function of "open" detector 15. The energy axis is in units of the k-edge of the fluorescer of detector 1, E0. All energy units in this study are given in units of E0.

FIGURE I: Example of an "open" response function

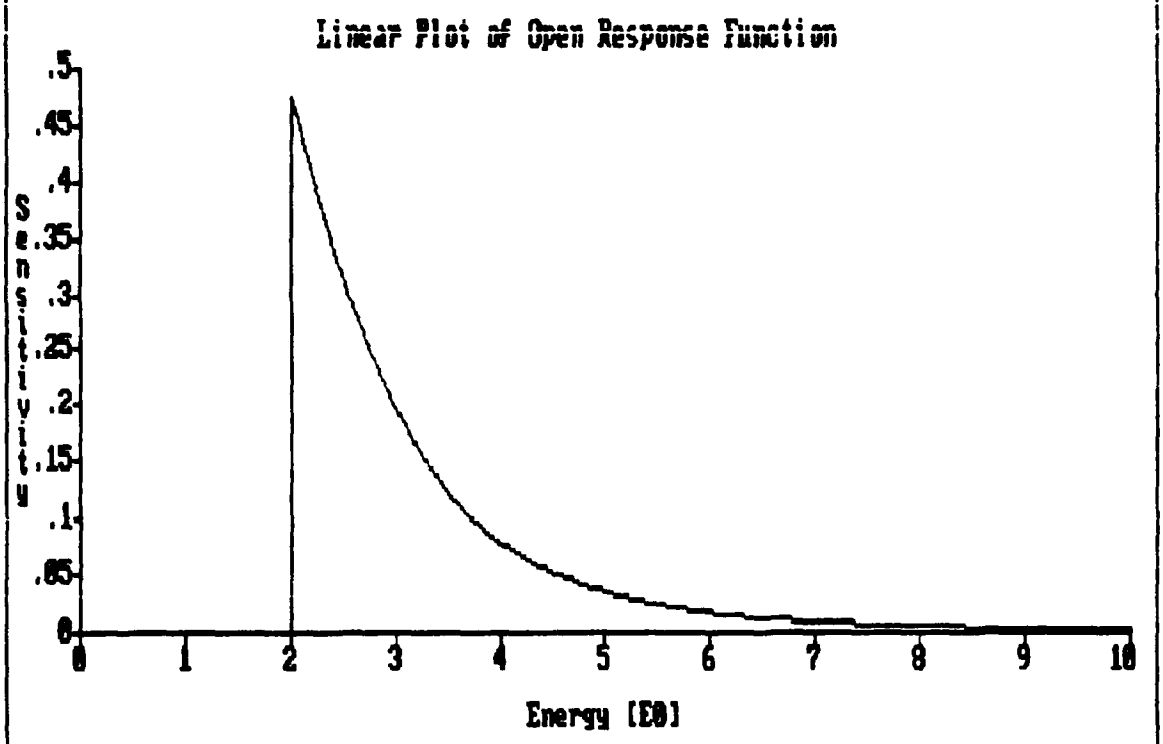

The "closed" detector system is a filter-fluorscer detector which shapes the "open" detector-type response into a more pulse-like envelope. This envelope, or inband response, is between the k-edges of the filter and the fluorescer. Both detector systems studied are asymmetric.

The equation for the closed response function (3:3-3) is given by:

$$R_i^{closed}(E) = \begin{cases} 0 \quad for \quad E < E_i^0 \\ \left(\frac{1}{E}\right)\left\{1-\exp\left[-2\left(\frac{E_i^0}{E}\right)^3\right]\right\}\exp\left[-0.25\left(\frac{E_i^1}{E}\right)^3\right] \quad for \quad E_i^0 \le E < E_i^1 \\ \left(\frac{1}{E}\right)\left\{1-\exp\left[-2\left(\frac{E_i^0}{E}\right)^3\right]\right\}\exp\left[-1.5\left(\frac{E_i^1}{E}\right)^3\right] \quad for \quad E > E_i^1 \end{cases} \tag{5}$$

Figure II is an example of a closed response function. The sensitivity is the amplitude of the response function of "open" detector 15. The energy axis is in units of the k-edge of the fluorescer of detector 1, E0.

FIGURE II: Example of a "closed" response function

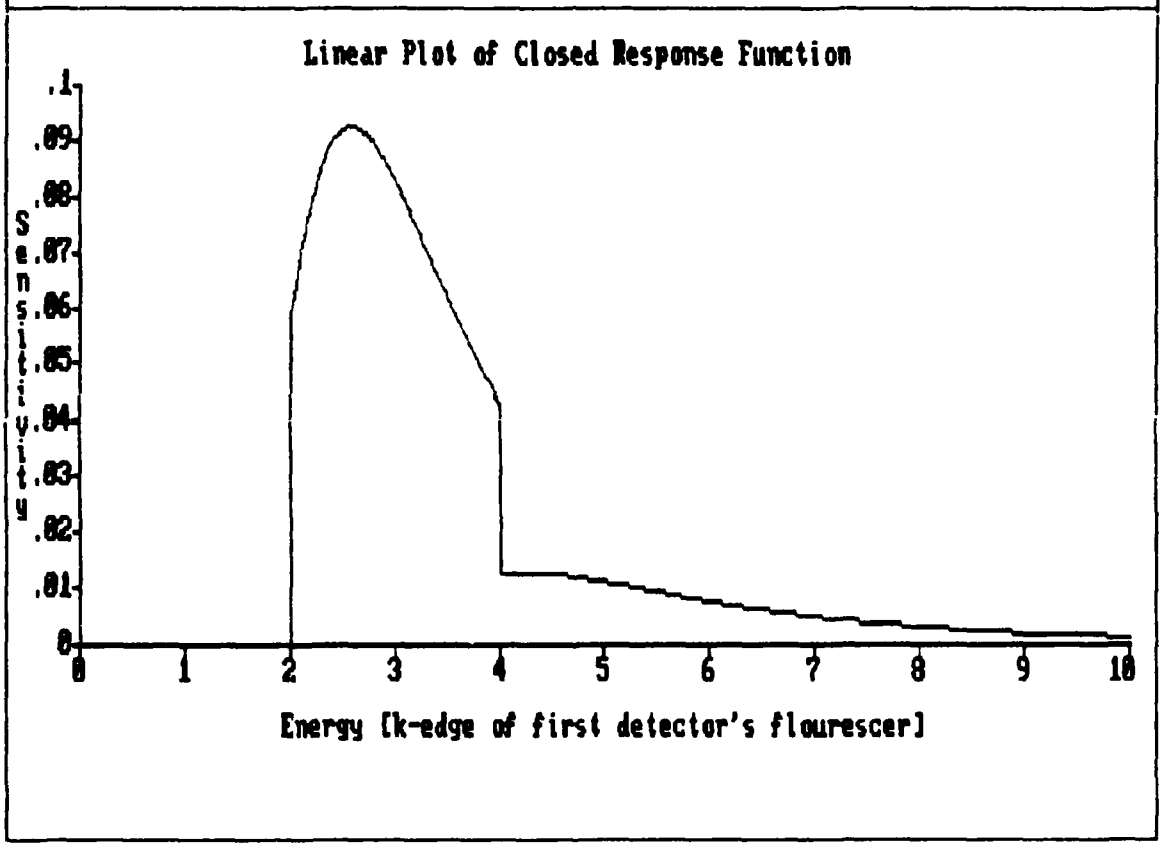

Both the "open" and "closed" response functions discussed above are ideal. In the presence of calibration and measurement errors, the real response function is perturbed in the following way:

$$\hat{R}_i(E) = R_i(E) + \Delta R_i(E) \qquad (6)$$

where

$\hat{R}_i(E)$ = the actual response function

$\Delta R_i(E)$ = the change in the response function due to calibration and measurement errors. This change could be negative giving a smaller value for the response function.

Definition of Spectra

Three spectra are used in this study: the predicted spectrum, the actual spectrum, and the unfolded spectrum. The predicted spectrum, $S_p(E)$, is the spectrum expected from theoretical calculations. This spectrum is known.

The actual spectrum, $S_a(E)$, is the spectrum to which the detectors respond. In the field tests, the actual spectrum is unknown and to some extent, unknowable. For the purpose of comparing the performance of the unfolding methods, $S_a(E)$ is chosen. The ability of the unfolding methods to recover $S_a(E)$ is the measure of the method's suitability.

The unfolded spectrum, $S_u(E)$, is calculated from detector output and response function data to be an approximation to $S_a(E)$. The predicted spectrum may be used as an initial guess for the unfolding methods.

Definition of Signals

A signal, Y_i produced by a spectrum s(E)dE, is the detector output given by the following equation:

$$Y_i = \int_0^\infty R_i(E)s(E)dE \qquad (7)$$

There are four signals associated with the three spectra already defined: the ideal signal, the measured signal, the predicted signal, and the unfolded signal. The ideal signal, Y_i^{ideal}, is the signal produced by the actual, but unknown, spectrum as measured by an ideal instrument. The ideal signal is unknown because of errors in calibration and uncertainties in measurement and detection. The ideal signal is given by:

$$Y_i^{ideal} = \int_0^\infty R_i(E)S_a(E)dE \qquad (8)$$

The measured signal, $Y_i^{measured}$, is the signal measured by the detectors with all the calibration errors and measurement and detection uncertainties included. The measured signal is given by:

$$Y_i^{measured} = \int_0^{\infty} \hat{R}_i(E) S_a(E) dE \qquad (9)$$

The predicted signal, $Y_i^{predicted}$, is the signal expected from the predicted spectrum as measured by the ideal instrument. The predicted signal is given by:

$$Y_i^{predicted} = \int_0^{\infty} R_i(E) S_p(E) dE \qquad (10)$$

Finally the unfolded signal, $Y_i^{unfolded}$, is the signal that would be produced by the unfolded spectrum as measured by the ideal instrument. The unfolded signal is given by:

$$Y_i^{unfolded} = \int_0^{\infty} R_i(E) S_u(E) dE \qquad (11)$$

The signal data from underground nuclear effects simulations are frequently specified as a ratio to the predicted signal; it is in this form that the χ^2 test statistic will be formulated. The measured-to-predicted ratio is given by:

$$b_i \equiv \frac{Y_i^{measured}}{Y_i^{predicted}} \qquad (12)$$

and the unfolded-to-predicted ratio is given by:

$$c_i = \frac{Y_i^{unfolded}}{Y_i^{predicted}} \qquad (13)$$

Errors in the Measurement Process

There are two basic errors that occur during the measurement process: measurement error and calibration error. The measurement error is the uncertainty in the measurement of the detector output. This uncertainty includes errors introduced in the transmission of the signal, the recording of the signal, and the reading of the signal.

The calibration error is the uncertainty in the determination of the detector response function. Experiments are conducted to determine the detector response function by using known x-ray sources. These calibrations are subject to errors in the measurement process.

The experimenter accounts for these errors by the specifying a measurement standard deviation, σ_i for each of the detectors. These deviations are based on past experiments and detector calibrations.

Normal Distribution for Simulating Measurement Error

The measurement errors are assumed, in this study, to be normally distributed. They are simulated by random number sampling of a Gaussian probability distribution function, which is approximated by a sum of continuous uniform distributions i.e., a sum of random numbers. Let X be a random variable which is defined by:

$$X = \sum_{n=1}^{12} x_n - 6 \qquad (14)$$

where

$x_n \in U[0,1]$

$U[0,1]$ is a uniform distribution on the interval [0,1].

The mean for X is (8:565):

$$\mu_X = E[X] = E[12U[0,1] - 6] = 12E[U[0,1]] - 6 = 0 \qquad (15)$$

Since σ^2 for a uniform distribution of the interval [0,1] is given by the following (8:570):

$$\sigma^2 = \frac{1}{12} \qquad (16)$$

and the standard deviation is (8:566):

$$\sigma_X = \sigma_{12U[0,1]-6} = 12\sigma_{U[0,1]} = 12 \cdot \frac{1}{12} = 1 \qquad (17)$$

then

$$X \approx G(\mu = 0; \sigma = 1) \qquad (18)$$

which is the standard normal distribution.

Definition of Unfolding Methods

Given that the measured signal ($Y_i^{measured}$), predicted spectrum ($S_p(E)$), and the response functions for the detectors ($R_i(E)$) are known, then the problem is to solve for the actual spectrum, $S_a(E)$, in the system of equations:

$$Y_i^{measured} \approx \int_0^{\infty} R_i(E) S_a(E) dE \qquad (19)$$

However this problem is ill-posed (6:175), in that there are an infinite number of spectra, $S_a(E)$, which will satisfy this equation. So additional assumptions are imposed to determine a unique solution, $S_u(E)$, such that $su(E) \approx sa(E)$. The unfolded signals should equal, or at least approximate, the measured signals. The closeness of the approximation depends on the estimation of the accuracy of the measurement and is discussed below. So,

$$Y_i^{measured} = \int_0^{\infty} \hat{R}_i(E) S_a(E) dE \approx \int_0^{\infty} R_i(E) S_u(E) dE \qquad (20)$$

or, in order to solve numerically

$$Y_i^{measured} = \sum_{k=0}^{k_{max}} \hat{R}_{i,k} S_{a_k} \Delta E_k \approx \sum_{k=0}^{k_{max}} R_{i,k} S_{u_k} \Delta E_k \qquad (21)$$

The other constraints are dependent upon the method of solving for Su(E).

Basis Function Method

There are three methods, examined in this study, to compute a "reasonable" spectrum for $S_u(E)$: basis function(s) expansion, iteration of a better fit and smoother operation, and iteration of a better fit using a smoothed response function. The basis function expansion, with Plankian and cubic spline basis functions, was studied by Daniel (3:1-4). The idea is to approximate $S_a(E)$ as a sum of basis function(s), so $S_a(E)$ is chosen to satisfy:

$$S_a(E) = \sum_{j=1}^{j_{max}} \alpha_j B_{j,k} \qquad (22)$$

where

j = summation index over basis functions

$B_{j,k} = B_j(E;\vec{q})$ is the basis function j

$\vec{q}$ = the defining parameters for B_j

The parameters, $\vec{q}$, define the basis function and are dependent upon the type of basis function. For Plankian basis functions these parameters reduce to a single value, the temperature of the Plankian. However, for cubic splines, the parameters include the locations of the knots and the temperature of the Plankian fit between the next-to-last and last knots.

Substituting Equation (22) into Equation (21) gives,

$$Y_i^{unfolded} = \sum_{k=0}^{k_{max}} R_{i,k} \sum_{j=1}^{j_{max}} [\alpha_j B_{j,k}] \Delta E_k \qquad (23)$$

or rearranging,

$$Y_i^{unfolded} = \sum_{j=1}^{j_{max}} \alpha_j \hat{B}_{i,j} \qquad (24)$$

where

$$\hat{B}_{i,j} = \sum_{k=0}^{k_{max}} R_{i,k} B_{j,k} \Delta E_k \qquad (25)$$

In this method, a guess is made for the initial unfolded spectrum by specifying the parameters (α_j *and* $\vec{q}$) and number of basis functions (j_{max}). As a consequence $B_{j,k}$ can be determined and since $R_{i,k}$ and ΔE_k are known then $\hat{B}_{i,j}$ can be calculated. Finally $Y_i^{unfolded}$ can be evaluated by using Equation (24), .

This initial guess is modified, by changing α_j and/or $\vec{q}$ to minimize the χ^2 difference between $Y_i^{unfolded}$ and $Y_i^{measured}$. The method is terminated when the χ^2 test statistic of the difference is sufficiently small. I.e.,

$$\chi^2(Y_i^{measurement}, Y_i^{unfolded}) < \chi^2_{acceptable} \qquad (26)$$

The formulation of the χ^2 test statistic is discussed below.

Iteration Method

The second procedure, to compute a reasonable $S_u(E)$, is the iterative method. The iterative method is the repeated application of two spectrum changing operations: the "better fit" and "smoother". The "better fit" algorithm forces the unfolded signal, for the energy interval E to $E+dE$, to equal that of the measured spectrum:

$$R_i(E)s^{measured}(E)dE = R_i(E)s^{unfolded}(E)dE \qquad (27)$$

This is accomplished by scaling the guessed spectrum, for that energy interval, by the ratio of the measured to unfolded signal.

$$R_i(E)s_u^{\left(n+\frac{1}{2}\right)}(E)dE = \frac{Y_i^{measured}}{Y_i^{unfolded}} R_i(E)s_u^{(n)}(E)dE \qquad (28)$$

where,

$s_u^{\left(n+\frac{1}{2}\right)}(E)dE$ is better-fit of interation n of the unfolded spectrum.

$s_u^{(n)}(E)dE$ is iteration n of the unfolded spectrum.

Equation (28) can be rewritten by using Equations (12) and (13):

$$R_i(E)s_u^{\left(n+\frac{1}{2}\right)}(E)dE = \beta_i R_i(E)s_u^{(n)}(E)dE \qquad (29)$$

where

$$\beta_i = \frac{\int_0^\infty \hat{R}_i(E) S_a(E) dE}{\int_0^\infty R_i(E) S_u(E) dE} \approx \frac{Y_i^m}{Y_i^u} = \frac{Y_i^m / Y_i^p}{Y_i^u / Y_i^p} = \frac{b_i}{c_i} \quad (30)$$

For the underground nuclear effects simulations, the detectors are designed to have overlapping energies to reduce calibration and measurement errors. So, the total unfolded signal for an energy interval for all the detectors is given by

$$\sum_{i=1}^{i_{max}} R_i(E) S_u^{\left(n+\frac{1}{2}\right)}(E) dE = \sum_{i=1}^{i_{max}} \beta_i R_i(E) S_u^{(n)}(E) dE \quad (31)$$

but $S_u^{\left(n+\frac{1}{2}\right)}(E)dE$ and $S_u^{(n)}(E)dE$ are not dependent upon the detector index so,

$$\left[\sum_{i=1}^{i_{max}} R_i(E)\right] S_u^{\left(n+\frac{1}{2}\right)}(E) dE = \left[\sum_{i=1}^{i_{max}} \beta_i R_i(E)\right] S_u^{(n)}(E) dE \quad (32)$$

finally, the effect of the "better fit" on the last spectrum is given by:

$$S_u^{\left(n+\frac{1}{2}\right)}(E) dE = \frac{\left[\sum_{i=1}^{i_{max}} \beta_i R_i(E)\right]}{\left[\sum_{i=1}^{i_{max}} R_i(E)\right]} S_u^{(n)}(E) dE \quad (33)$$

The detector response functions, $R_i(E)$, have discontinuities about the k-edges of its filter and flourescer, FIGURES I and II. During the "better fit" algorithm, the scaling factor in Equation (33) can be significantly different even between adjacent detectors.

FIGURE III gives an illustration of such a case, the obvious discontinuities are at 16 and 24 E_0. Unrealistic features that are a function of the method, such as the discontinuous slope, are called an artifact of the method.

FIGURE III: Example of discontinuities after a better-fit operation

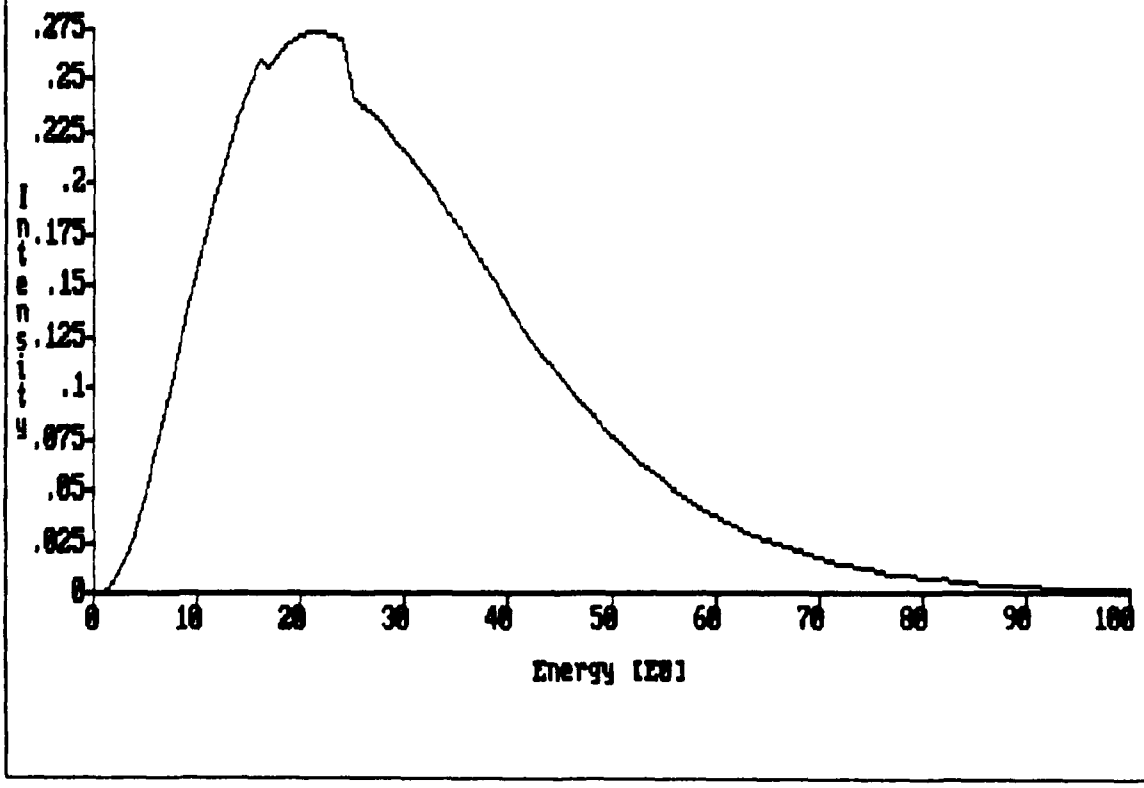

The second spectrum-modifying operation of the iteration method, the "smoother", is designed to spread-out the artifact of the "better-fit" algorithm so that the resulting spectrum is more realistic.

The averaging of the artifacts with the surrounding spectrum, is done in the following manner:

$$S_u^{(n+1)}(E)dE = \frac{\int_0^\infty f(E,E')S_u^{\left(n+\frac{1}{2}\right)}(E')dE'}{\int_0^\infty f(E,E')dE'}dE \qquad (34)$$

or written to be solved numerically,

$$S_k^{(n+1)}dE = \frac{\sum_{k'=1}^{k_{max}} f_{k,k'}S_{k'}^{\left(n+\frac{1}{2}\right)}\Delta E_{k'}}{\sum_{k'=1}^{k_{max}} f_{k,k}\,\Delta E_{k'}}dE \qquad (50)$$

produces a spectrum that is nearer to $S_a(E)dE$ than $S_u^{\left(n+\frac{1}{2}\right)}(E)dE$.

There were several constraints placed upon the averaging kernel, $f_{k,k'}$, during this study. For computational ease, the kernel was normalized i.e., for all E

$$\int_0^\infty f(E,E')dE' = 1 \qquad (36)$$

or for discrete energy bins,

$$\sum_{k=1}^{k_{max}} f_{k,k'} \Delta E_{k'} = 1 \tag{37}$$

This simplifies Equation (50) to

$$S_k^{(n+1)} dE = \left[\sum_{k'=1}^{k_{max}} f_{k,k'} S_{k'}^{(n+\frac{1}{2})} \Delta E_{k'} \right] dE \tag{38}$$

The second constraint imposed on $f_{k,k'}$ is that $f_{k,k'}$ is symmetric about k i.e., for constant energy bins:

$$f_{k,k-\delta k} = f_{k,k+\delta k} \tag{39}$$

This is equivalent to saying that the averaging algorithm does not favor higher or lower energies. For energy bins that are geometrically spaced i.e., for any k the following is true:

$$E_{k+1} = r E_k \tag{40}$$

where r is a constant, then the symmetry of $f_{k,k'}$ is expressed as:

$$f_{k,k/r} = f_{k,rk} \tag{41}$$

Finally because $f_{k,k'}$ is symmetric about k, a symmetric difference kernel was often used to improve the computational efficiency of the "smoothing" algorithm i.e.,

$$f_{k,k'} = f_{|k-k'|} \tag{42}$$

This changes Equation (55) to the following:

$$S_k^{(n+1)} dE = \sum_{k'=-\delta k_{max}}^{\delta k_{max}} f_{|k-k'|} S_{k'}^{\left(n+\frac{1}{2}\right)} \Delta E_{k'} dE \tag{43}$$

This is generally much easier to compute because the interval $[-\delta k_{max}, \delta k_{max}]$ of Equation (58) is much smaller than the interval $[1, k_{max}]$.

The iteration method is employed in the following way. An initial spectrum, $S_{guess}(E)dE = S_u^{(0)}(E)dE$, is guessed. The "better-fit" algorithm, Equation (49) is applied to $S_u^{(0)}(E)dE$ to produce $S_u^{\left(n+\frac{1}{2}\right)}(E)dE$. The smoother, Equation (58), is then applied to produce $S_u^{(1)}(E)dE$, the first iteration. At this point, a judgement would have to be made to evaluate if the first iteration is reasonable. If it is, then the first iteration is the answer. If not, then the iteration method is reapplied until one of the spectra is reasonable.

In practice, the "better-fit" and "smoother" algorithms compete against each other; the "better-fit" pushes the unfolded spectrum toward the actual spectrum while the "smoother" pushes the unfolded spectrum away. This leads to the last assumption for the iteration method:

The final unfolded spectrum, which is a compromise between the "better fit" and "smoother" algorithms, is a good approximation to the actual spectrum. I.e., there is a best N (which should appear in the early iterations) such that:

$$S_u^{(N)}(E)dE \approx S_a(E)dE \tag{44}$$

The third method is the iteration of a better fit using a response function smoothed only around the k-edges. This method is related to the second method, with the "smoother" algorithm buried in the initial smoothing of the response function. However, in this case, the "smoother" is local and weak compared to the "better fit" algorithm, so the overall effect is primarily due to the "better fit" algorithm.

Modified Iteration Method

In order to remove artifacts yet not work against the "better-fit" algorithm, a third method is discussed which is a modification of the iteration method. The modified iteration method works as follows: the response function is smoothed only around the k-edges of the detectors i.e.,

$$R^s_{i,k} = \sum_{k'=-\delta k_{max}}^{\delta k_{max}} f_{|k-k'|} R_{i,k} \Delta E_k \tag{45}$$

and then normalized. In other words, the "smoother" has already been used on the response function to prevent the discontinuities during the "better-fit" algorithm. The "better-fit" algorithm now has the following modified form:

$$S_u^{(n+1)}(E)dE = \left[\sum_{i=1}^{i_{max}} \alpha_i R_i(E)\right] S_u^{(n)}(E)dE \qquad (46)$$

Most of the previous discussion of the iteration method also applies to the modified iteration method.

Errors in the Unfolding Process

There are two errors associated with the unfolding process: approximation of an integral by a summmation and the ill-posedness of the Fredholm integral equation. Whenever an integral is replaced by a summation in order to be numerically computed there is an error associated with the replacement:

$$\int_0^\infty R_i(E)s(E)dE = \sum_{j=1}^{j_{max}} R_{i,j}s_j\Delta E_j + \delta \qquad (47)$$

where,

$$R_{i,j} = R_i\left(E_j + \frac{\Delta E_j}{2}\right)$$

δ is the error associated the approximation

δ is dependent upon the bin size, ΔE_i.

Another error is due to the ill-posedness of the Fredholm integral equation. Because the Fredholm integral equation of the first kind is ill-posed, there are an infinite number of the solutions that satisfy the integral i.e.,

$$\int_0^\infty R_i(E)s_1(E)dE = \int_0^\infty R_i(E)s_2(E)dE \qquad (48)$$

doesn't guarantee that $s_1(E) = s_2(E)$. The spectrum determined is dependent upon the unfolding method.

The actual spectrum is not expected to be determined by the any of the methods presented here. The unfolding methods produce a particular solution to the integral equation which has a reasonable shape e.g., a continuous slope everywhere. Different methods can be used to produce reasonable shapes and some of the methods will produce reasonable shapes for certain detector signals.

Flux Non-negativity Constraints

Negative intensity, for radiation, is meaningless. However during the unfolding process, the spectra can become negative at some energies. So a non-negativity constraint is applied such that:

$$S_u(E) = \begin{cases} 0 & \text{for } S'_u(E) \le 0 \\ S'_u(E) & \text{for } S'_u(E) > 0 \end{cases} \qquad (49)$$

Formulation of χ^2 Test Statistic

The test statistic used in terminating the basis function method uses the "goodness of fit" test of the measured-to-predicted ratios, b_i, to the unfolded-to-predicted ratios, c_i, and is given by:

$$\chi^2 = \sum_{i=1}^{instruments} \left(\frac{c_i - b_i}{\sigma_i} \right)^2 \qquad (50)$$

where

σ_i = the standard deviation of the measured-to-predicted ratio, b_i, based on estimates of detector calibration and measurement uncertainties.

When

$$\chi^2 \approx \nu \qquad (51)$$

where

ν = number of degrees of freedom of the unfolding method

then the unfolded and measured spectra are statistically equivalent. For the basis function method, the number of degrees of freedom is the number of parameters describing the basis function(s) i.e., a_i and $\vec{q}_i$.

Minimization of χ^2 Test Statistic

To improve the fit of the unfolded spectrum calculated by the basis function method, there is a systematic method to minimize χ^2 by varying the coefficients and parameters: a_i and $\vec{q}_i$. The Flecher-Powell (F-P) minimization technique was used to determine the approximate direction of the minimum for χ^2 in the basis functions' parameter space. The F-P technique takes an initial point, P, in the parameter space (which is determined by the unfolded spectrum) and calculates the direction in the following way:

$$S' = -H\nabla\chi^2(P) \tag{52}$$

then the unit normal direction is given by,

$$S = \frac{S'}{|S'|} \tag{53}$$

where H is initially a unit matrix of the parameter space.

Once the direction, S, has been approximately determined by the F-P technique then an appropriate distance, w, in the parameter space has to be determined to minimize χ^2. This is determined in the following manner:

the point, P, in parameter space has a value of $\chi^2(P)$ and a slope of $(\partial/\partial w)[\chi^2(P)]$ along the direction S. A small step, w', is taken along S from P to a new point, $P + w'S$. The value, $\chi^2(P + w'S)$, and the slope $(\partial/\partial w)[\chi^2(P + w'S)]$ are determined at the new point. With the two points and slopes, a cubic fit approximating the slice in parameter space can be calculated and a reasonable distance, w, is determined for the closest approach to the minimum along that slice.

FIGURE IV: Minimization by the Fletcher-Powell Technique

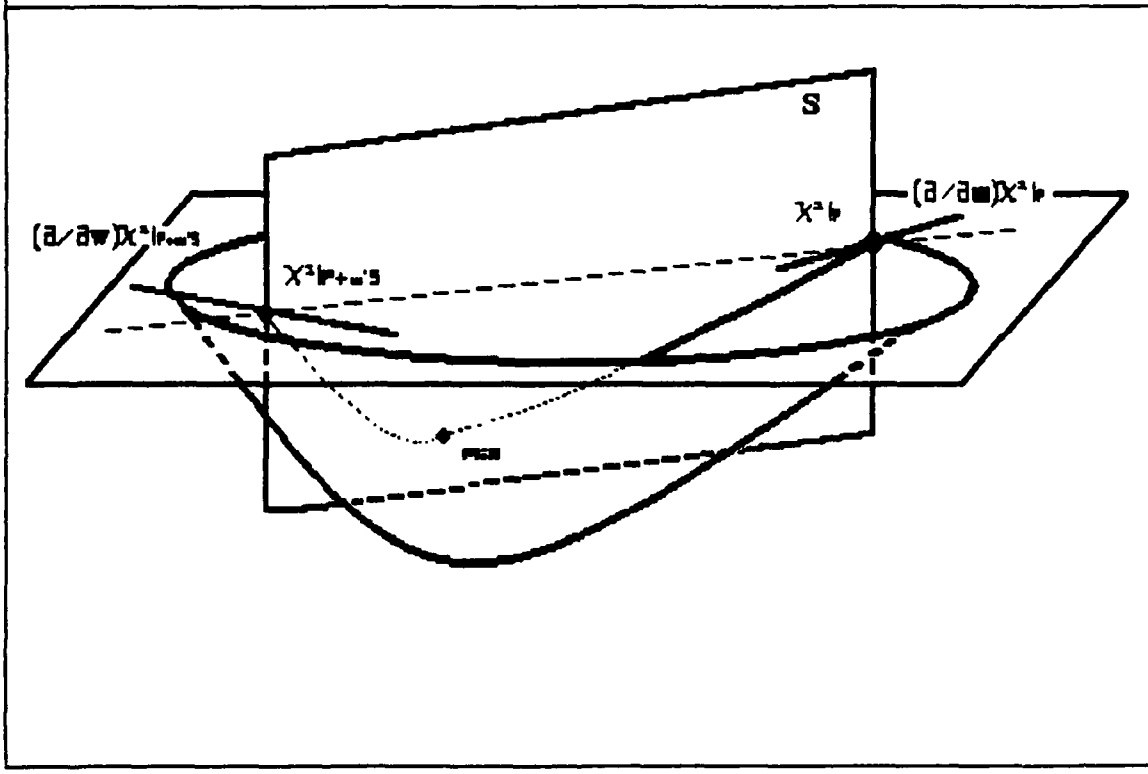

For the next use of the F-P technique, the unit matrix H is changed toward the minimum by the following formulae (6:76):

$$H = H + A - B \tag{54}$$

where

$$A = \frac{R R^T}{R^T Q} \tag{55}$$

$$B = \frac{H Q Q^T H}{Q^T H Q} \tag{56}$$

$$R = \chi^2(P + w' S) - \chi^2(P) \tag{57}$$

$$Q = (\partial / \partial \dot{w}) \chi^2 |_{P + w' S} - (\partial / \partial \dot{w}) \chi^2 |_P \tag{57}$$

If χ^2 is still too large, then the F-P technique is reapplied until the result is small enough.

III. Computer Program Implementation

Introduction

With the theoretical background developed, we can now discuss implementation of the unfolding algorithm. In this section, programming considerations are discussed.

Input of the Test Data

Data provided by a nuclear effects test includes: the predicted spectrum, $S_p(E)$, the calibrated detector response functions, $R_i(E)$, the measured-to-predicted ratios, b_i, and the detector standard deviations, σ_i. These variables are simulated by specifying them in a self-consistent manner.

$R_i(E)$ is assumed to be exact and given by Equations (4) and (5). The modified iteration method alters these response functions as part of its unfolding process, however the original response functions are used in the calculation of the χ^2 test statistic.

The detectors' standard deviation is specified as 0.15 by compatibility with Daniel's initial assumptions (3:1-3). Further discussion of the measurement error is covered in section II.

In reality, the predicted spectrum is based upon theoretical treatment of the physics of the actual simulation configuration and results from past simulations. This spectrum should be a very good approximation of the actual spectrum, which is unknown. For this study, the predicted specta

are always a good approximation to the actual spectra.

Although the measured-to-predicted ratios could have been chosen directly, the specification of the actual spectrum and calculating b_i with Equations (10), (11), and (12) allow a direct comparison of $S_a(E)$ to $S_u(E)$.

Basis Functions

Each of the spectra can be specified either as a basis function or explicitly listed data in a file. There are two types of basis functions used in this study: Planckians and cubic splines. The Planckian basis functions, $B_{j,k}$, as used in Equation (24) are written as:

$$B_{j,k} = \frac{15}{\pi k T^4} \frac{E^3}{\exp\left(\frac{E}{kT}\right) - 1} \tag{58}$$

where,

E = center bin energy in units of E_0

T = temperature of Plankian in units of E_0

k = Boltzmann's constant

The cubic spline basis functions are a composite of four cubic splines connecting each knot to it's surrounding knots. Each of the splines are given by the Lagrangian function:

$$L_{4,k}(E) = \prod_{i=0,\, i \neq k}^{4} \frac{E - knot_i}{knot_k - knot_i} \qquad (59)$$

where,

E = center bin energy, in units of E_0

$knot_i$ = energy of a surrounding knot, in units of E_0

$knot_k$ = energy of the reference knot, in units of E_0

The first, second, and last knots are located at 0, E_0, $10E_0$ respectively, with the weights of the first and last knots always set to 0. Modifications are used for knots near the edges of the energy interval.

If $knot_k$ has adjacent knots that are the first or second to last then, because a cubic spline could not be calculated to join the remaining knot, they are joined by linear curves. The second-to-last and the last knots are joined by a Planckian for the same reason.

Iteration Method

The iteration methods use two different schemes to smooth out the spectrum after the better-fit algorithm, flat-averaging and normal-averaging. The flat-averaging method gives equal weighting for all energy bins within the specifed interval. The normal-averaging method gives a normal weighting of the energy bins about a specified point.

Both methods compensate for intervals too close to the end of the

energy interval (E0 to 128E0) by truncating the long side of the averaging interval so that it is symmetric about the central point of the interval. Otherwise the smoothing function would bias the unfolded spectrum unrealistically away from the ends of the energy interval. The two smoothing schemes incorporate the possibility of nonconstant spacing.

In order to reduce the run time of the iteration method, the linear spacing of the energy bins was changed to a geometric spacing. This reduced the time to calculate the integrals involved in the measured-to-predicted and unfolded-to-predicted ratios. The overall run time was reduced by a factor of seven.

The modified iteration and basis function methods were left with linear energy bin spacing. This was done for the following reasons. The other unfolding methods, with linear spacing, had comparable running times to the geometric energy spacing version of the iteration method. The linear spacing was kept as a check against the results of the iteration's geometric energy bin spacing.

The stopping point for the iteration methods is based upon the judgement of the person running the program. It is almost an art to stop the program when it has nearly converged to the actual spectrum, but has not gone too far as to completely smooth out the original data. For the purposes of comparison in this study, both iteration methods were stopped after five iterations. This is comparable to the number of iterations used in the field (7).

IV. Results and Discussion

Introduction

This Section covers the cases run using the unfolding program discussed in the last section. The topics covered are the following: the validation cases, the effect of noise on the validation cases, the tests cases, and the effect of noise on the test cases.

Validation Cases

The validation cases are to ensure that the program is running properly. A "perfect" unfolding technique would produce an unfolded spectrum is equal to the actual spectrum. This perfect reproduction of the original spectrum can not be required because of the ill-posedness of the Fredholm equation, as discussed in section II. However, the unfolded spectrum should be a close approximation to the actual spectrum. The initial guess for the unfolded spectrum was the same for the iteration, modified iteration, and the Planckian basis function methods.

For the iteration, modified iteration, and Planckian basis function methods, the validation cases consisted of three cases:

1. The actual and guessed spectra are different Planckians. This is to show that the method will produce unfolded spectra that converges toward the actual spectrum. The actual spectrum was T = 3E0 and coefficient = 0.75. The guessed spectrum was T = 2E0 and coeffient = 0.5.

2. The actual and guessed spectra are the same. This is to show how an initially correct guess is changed by the unfolding method. The actual and guessed spectra were T = 3E0 and coefficient = 0.75.

3. The actual spectrum is a two temperature Planckian spectrum and the guessed spectrum is a one temperature Plankian spectrum. The actual spectrum was T1 = 3E0, coefficient 1 = 0.75, T2 = 10, and coefficient 2 = 5. The guessed spectrum was T = 10 and coefficient = 10.

For case 1, the modified iteration method produced an unfolded spectrum that follows the actual spectrum, but has discontinuities near the k-edges of the response functions, FIGURE V. This is characteristic of the iteration method.

FIGURE V: Modified Iteration Method, Case 1

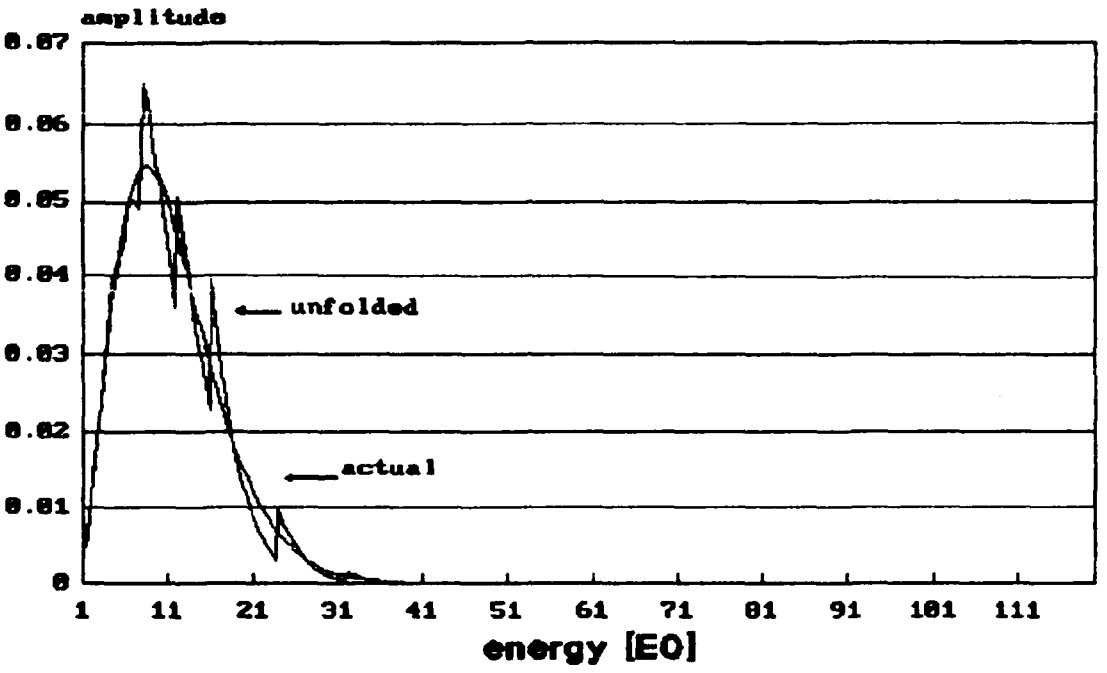

The unfolded spectrum from the iteration method had smoother and had less abrupt discontinuities than the modified iteration's solution did.

FIGURE VI: Iteration Method, Case 1

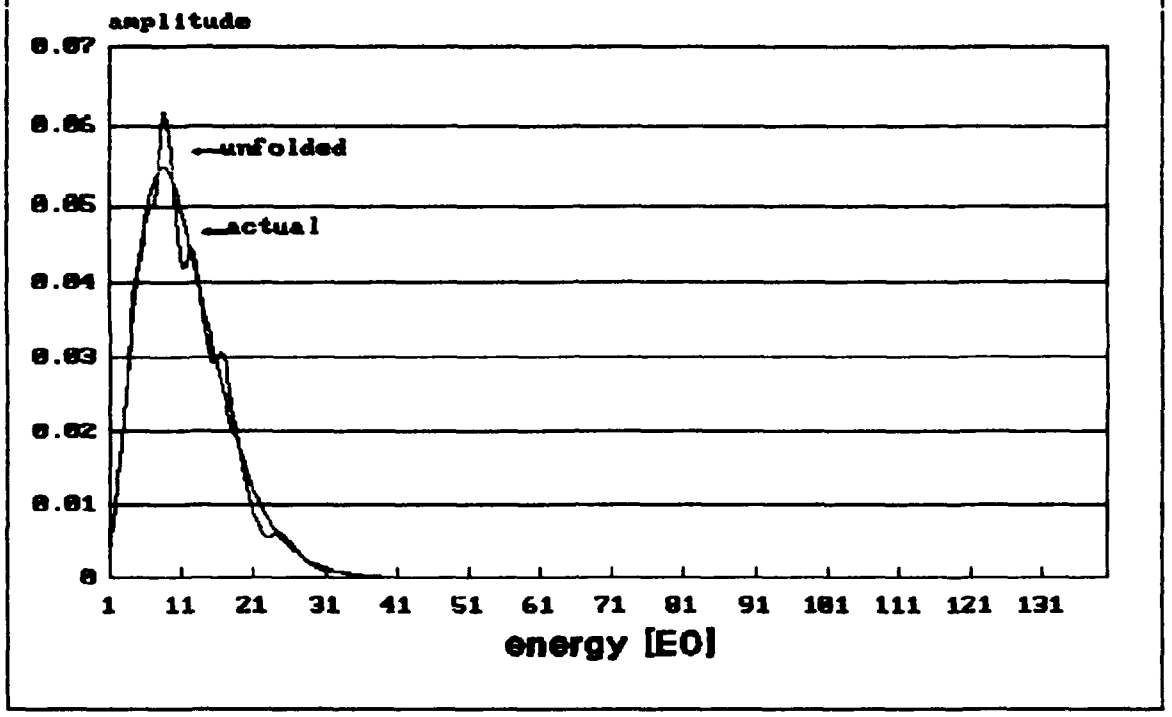

The Planckian basis function method gave an unfolded spectrum that appeared identical to the actual spectrum. All three methods successfully produced an unfolded spectrum which a good approximation to the actual spectrum, when the initial guess was wrong.

For case 2, both iteration methods and the Plankian basis function method produced an unfolded spectrum that was nearly identical to the actual spectrum (no figure was produced for this case because the spectra could not be distinguished). In other words, the unfolding methods didn't distort a correct guess.

For case 3, both iteration methods produced over-/under-shots for the greater energies, Figures VII. The Planckian method produced a good representation of the actual spectrum, as expected for a method to represent Planckian spectra.

FIGURE VII: Modified Iteration Method, Case 3

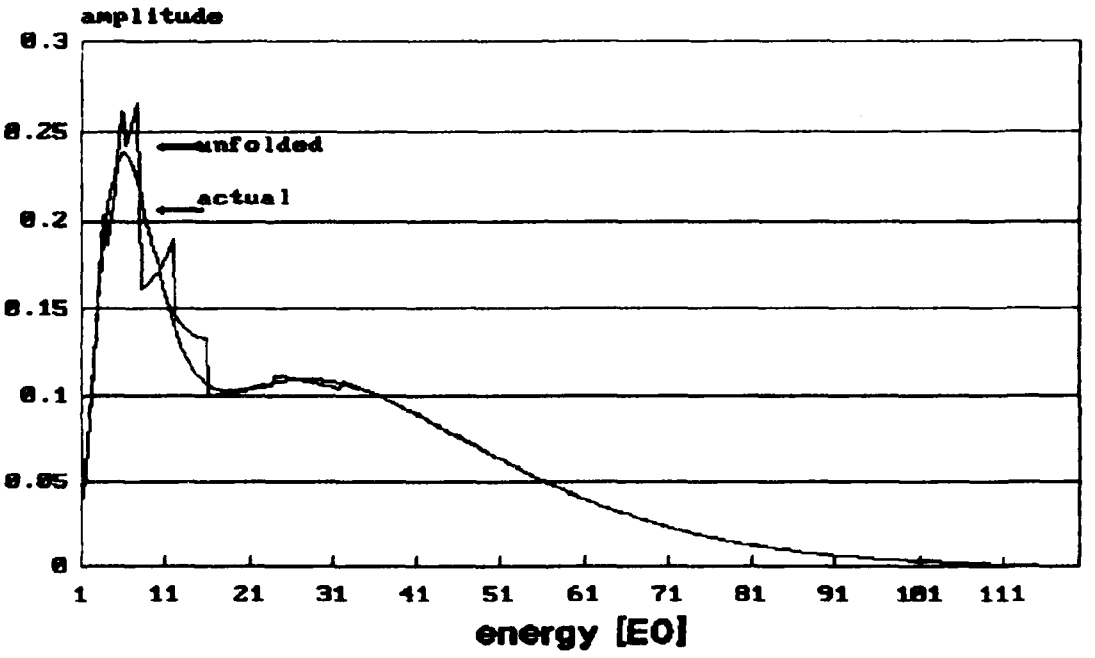

For the cubic spline, the validation cases consisted of two cases:

1. The actual and guessed cubic splines were different. The actual spectrum had six knots at the following locations: 0, E0, 5E0, 30E0, 60E0, and 128E0. The coefficients at these locations were 0, 5, 3, 2, 1, and 0, respectively. The temperature

of the Planckian curve joining the last two knots was 15E0.

The guessed spectrum had six knots at the following locations: 0, E0, 4E0, 35E0, 50E0, and 128E0. The coefficients at these locations were 0, 4, 4, 3, 2, and 0, respectively. The temperature of the Planckian curve joining the last two knots was 13E0.

2. The actual and guessed cubic splines were identical. The spectra have the same knot locations and coefficients as the actual spectrum of test case 1.

The cubic spline basis function method produced an unfolded spectrum, for each of the validation cases, that was nearly identical to the actual spectrum. However when the initial guess for the cubic spline basis function was chosen a little less carefully, the method didn't converge.

Effects of Errors on the Validation Cases

The effect of measurement and calibration errors was simulated by the addition of random numbers to the measured-to-predicted ratio, b_i, as discussed in the previous section. A demostration of this effect on the validation cases is illustrated by Figure X. In this figure, the modified iteration method was run in the presence of noise for case 2 (the guessed spectrum was correct). The collection of unfolded spectra has an envelope which follows the actual curve, but each unfolded spectrum has details which could have been interpreted as being significant.

FIGURE X: Modified Iteration with Noise, Case 2

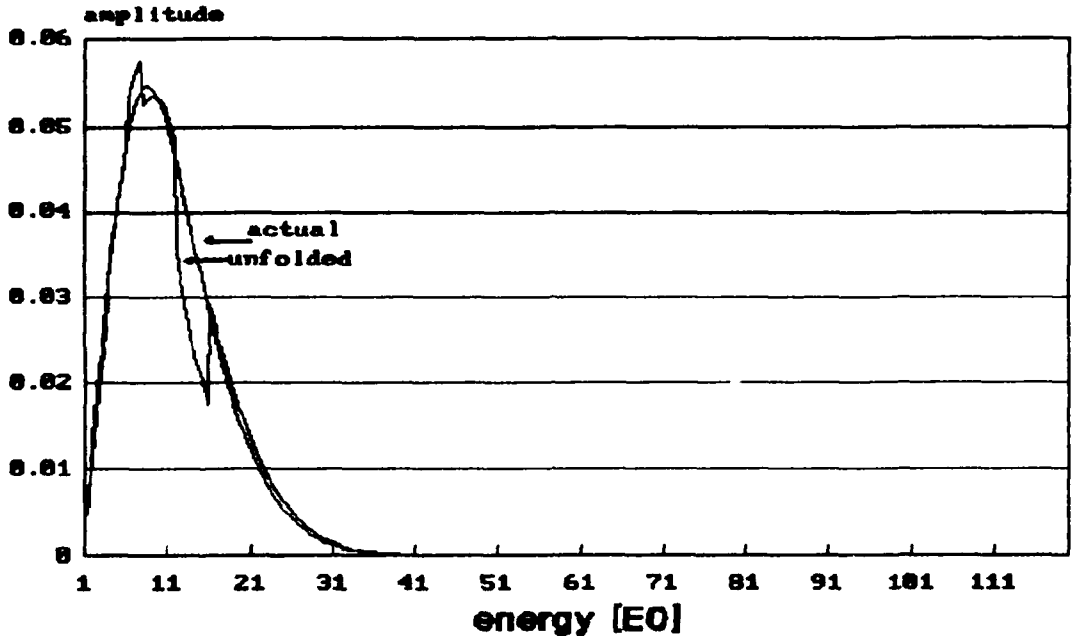

The dips in the unfolded spectra happened in the intervals where the noise from overlapping detectors were both negative. The peaks were where the noise from the overlapping detectors were both positive. When the noise was positive for one detector and negative for the overlapping detector, the overall effect of the noise was negligable.

There was another effect of the noise that was pecticular to the iteration method. The iteration method was run using a geometric spacing of the energy bins in order to significantly shorten the run times. For the iteration method for cases with no noise, the difference between the spectra using linear spacing and geometric spacing was negligable.

The noisy signal produced, for the geometric energy bins, very short spikes for small energies and long spikes for the larger energies. This is an artifact of the unfolding method. In order to give a realistic comparison for the noisy signal data produced by the iteration method, the linear energy bin spacing was used.

Test Cases

There were four actual spectra used to compare the unfolding methods. The following is a list of the actual spectra used for the test cases:

1. Two Planckians with a spike. This spectrum was chosen to compare the ability of the methods to recover broad structure (the two Plankians) with their ability to recover finer detail (the spike).

   The Planckians were T1 = 2E0, coefficient 1 = 2, T2 = 10E0, and coefficient 2 = 5. The spike was 11/8 E0 wide centered at 10E0.

   The guessed spectrum was the Planckian spectrum T = 10E0 and coefficient = 10. For the Planckian basis function method, a second two temperature Planckian was also used.

2. Heaviside function. This spectrum, and the following two, represent the ability of the unfolding method to represent discontinuous behavior of the actual spectrum. The actual

spectrum was 1 for energies less than 10E0 and 0.5 for energies greater than 10E0.

The guessed spectrum for all methods was 0.75 for all energies. The Plankian basis function wasn't used for this or the following two discontinuous actual spectra.

3. Barrier function. The actual spectrum was 1 between energies 8E0 and 12E0, but 0.5E0 for all other energies. The guessed spectrum, for all the methods, was 1 for all energies.

4. Triangle function. The actual spectrum was an isosceles triangle with an apex of 1 at 10E0 and a value of 0.5 at the base. The base extended from 6E0 to 14E0. The actual spectrum was 0.5 for all other energies. The guess spectrum, for all the methods, was 1 for all energies.

Both the modified iteration and iteration methods made an attempt to represent the spike by a broader shape at the same energy as shown in Figures XI and XII, respectively. The pulse seems to disrupt the spectrum for larger energies. This is probably due to the overlapping response functions in the energy range of the spike.

FIGURE XI: Modified Iteration, Test Case 1

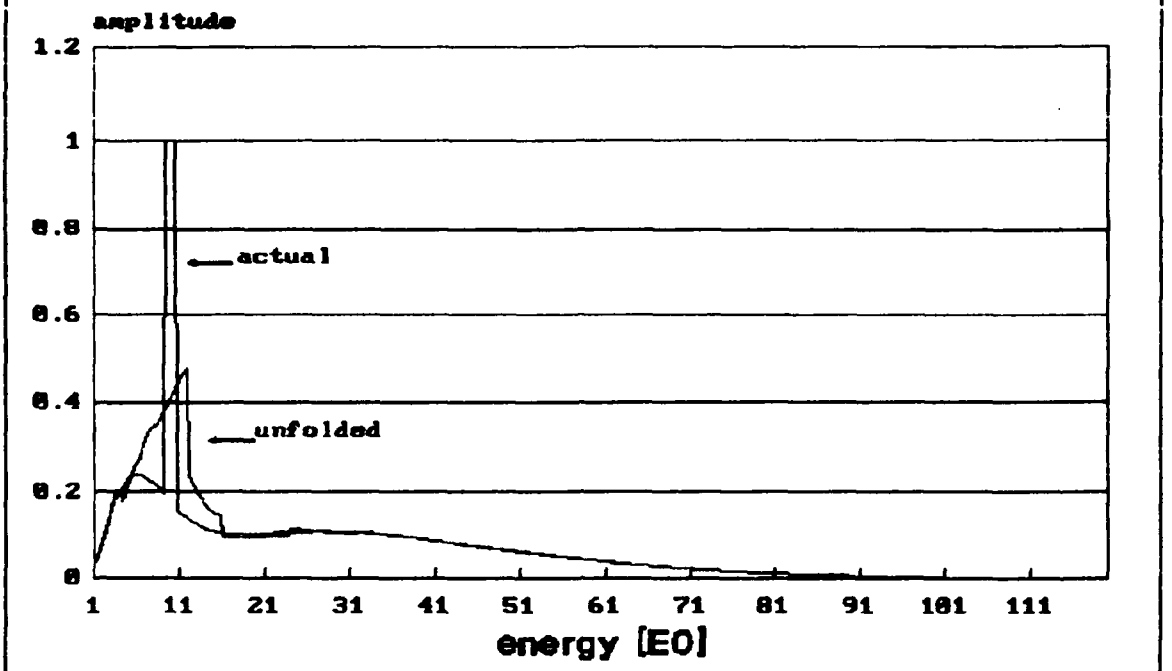

FIGURE XII: Iteration, Test Case 1

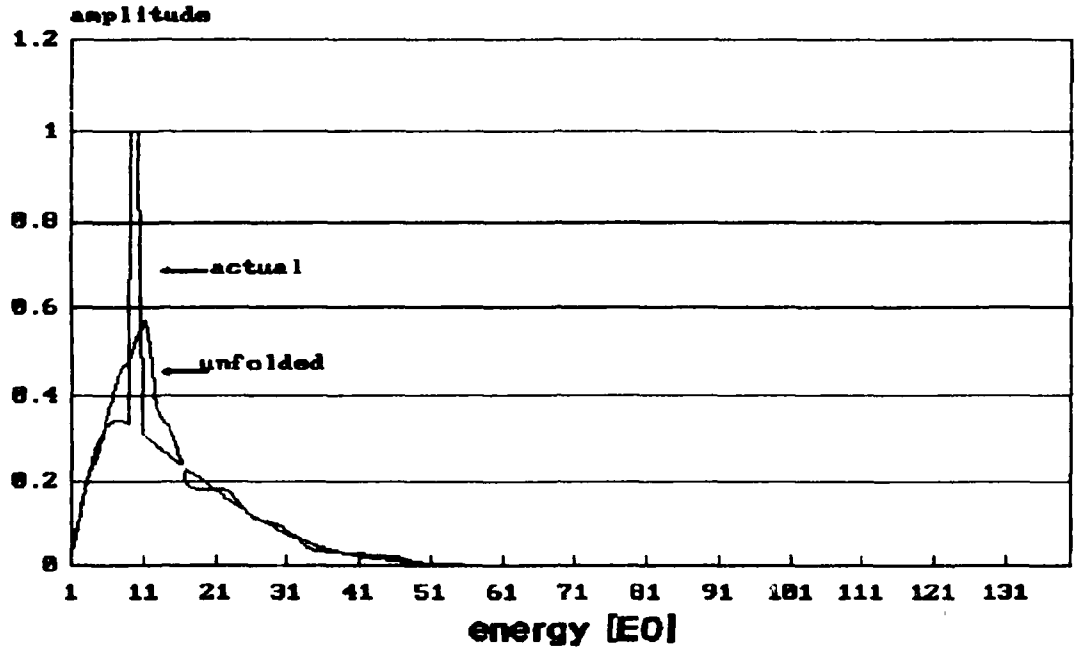

The Planckian basis function method produced an unfolded spectrum composed of two Planckians of different temperatures. Because of the relative temperatures and coefficients, the spectrum appears to be a one temperature Planckian as shown in Figure XIII.

FIGURE XIII: Planckian Basis Function, Test Case 1

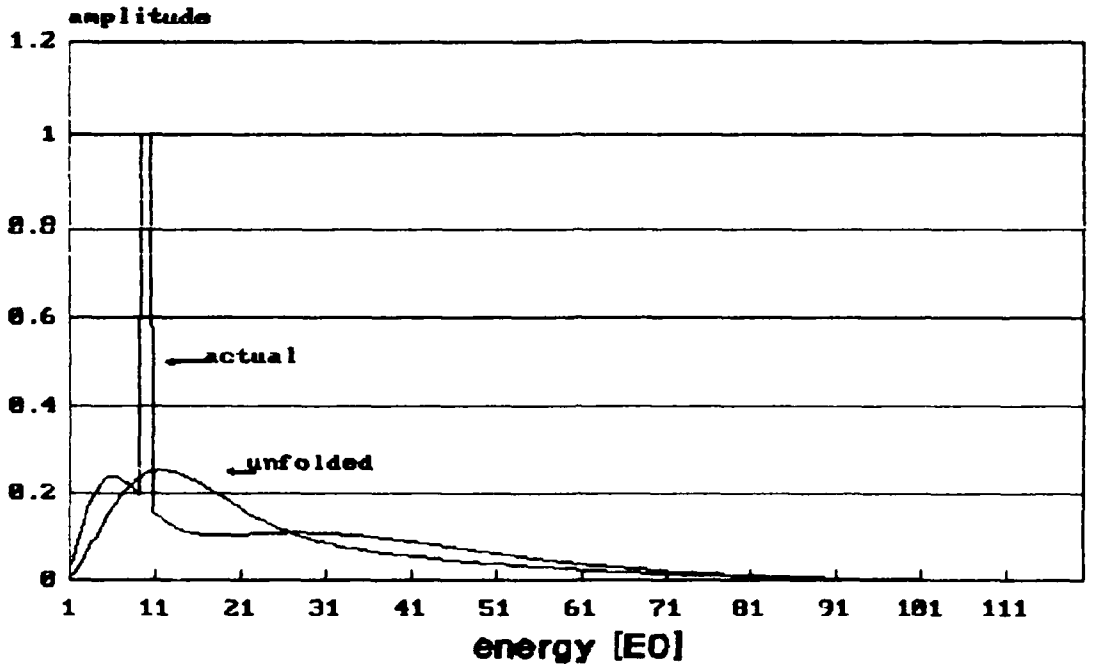

The two iteration methods have a ragged approximation to the Heaviside spectrum, rounding off the corners and crossing the discontinuity at the midpoint, Figure XIV and XV. For the cubic spline, the unfolded spectrum can't be distinguished from the actual spectrum. This is not unexpected as the cubic spline has a good ability to represent straight lines.

FIGURE XIV: Modified Iteration, Test Case 2

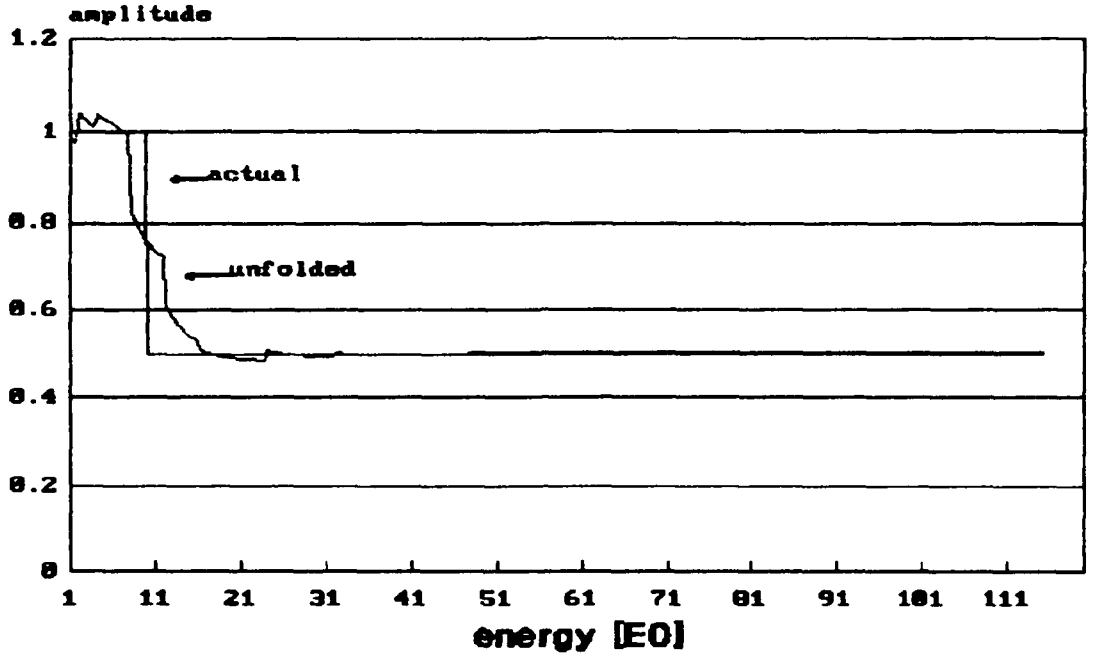

FIGURE XV: Iteration, Test Case 2

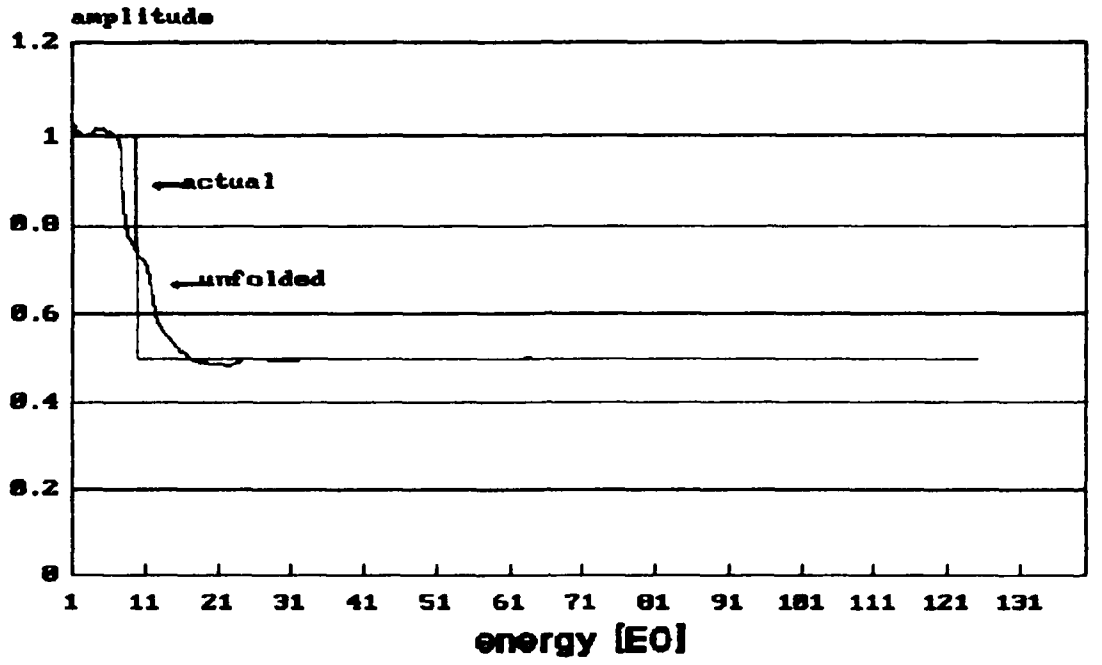

For test case 3, the two iteration methods move their unfolded spectra to follow the actual spectrum into the spike discontinuity, Figure XVI and Figure XVII. The cubic spline's unfolded spectrum with seven knots follows the discontinuous spike of the actual spectrum as shown in Figure XVIII. Except for the dropoff for the higher energies, the cubic spline is a better approximation than the iteration methods.

FIGURE XVI: Modified Iteration, Test Case 3

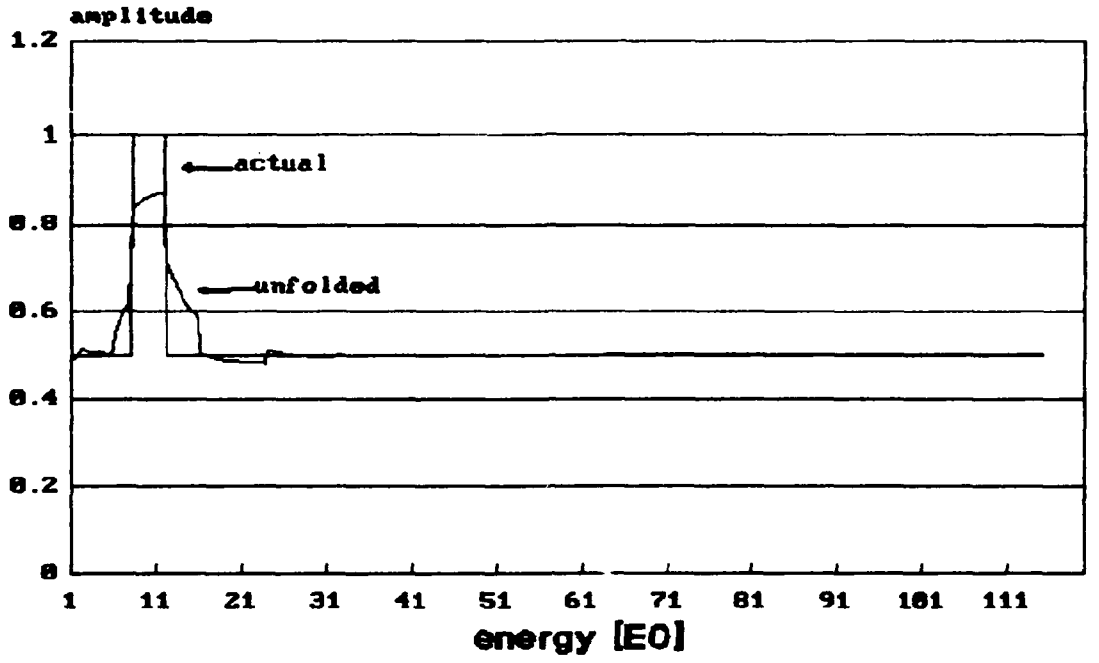

FIGURE XVII: Iteration, Test Case 3

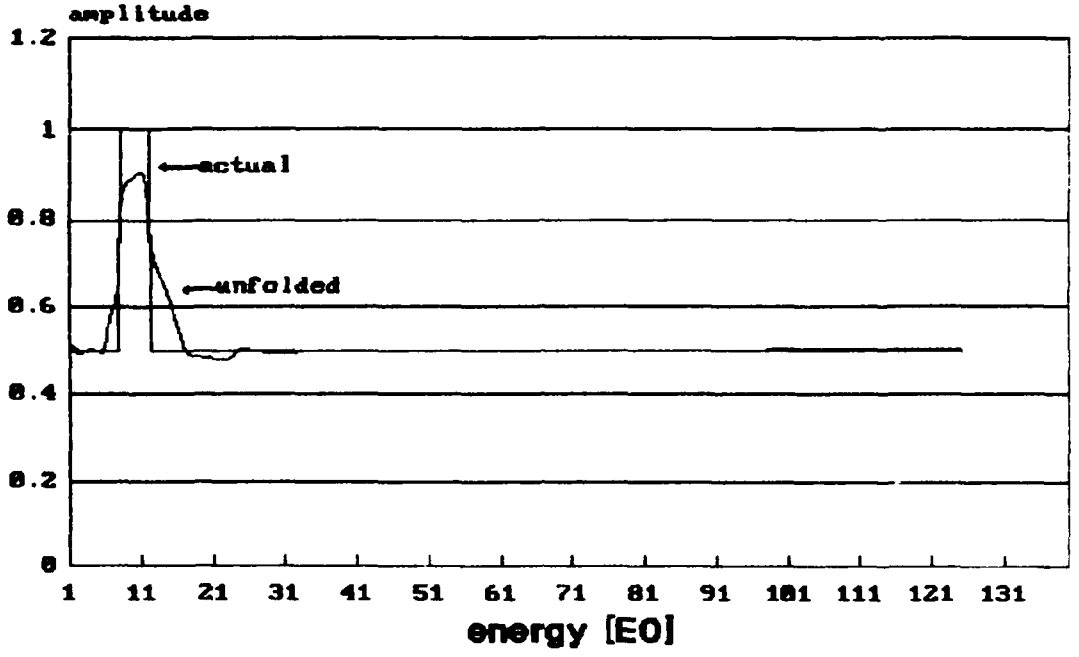

FIGURE XVIII: Cubic Spline, Test Case 3

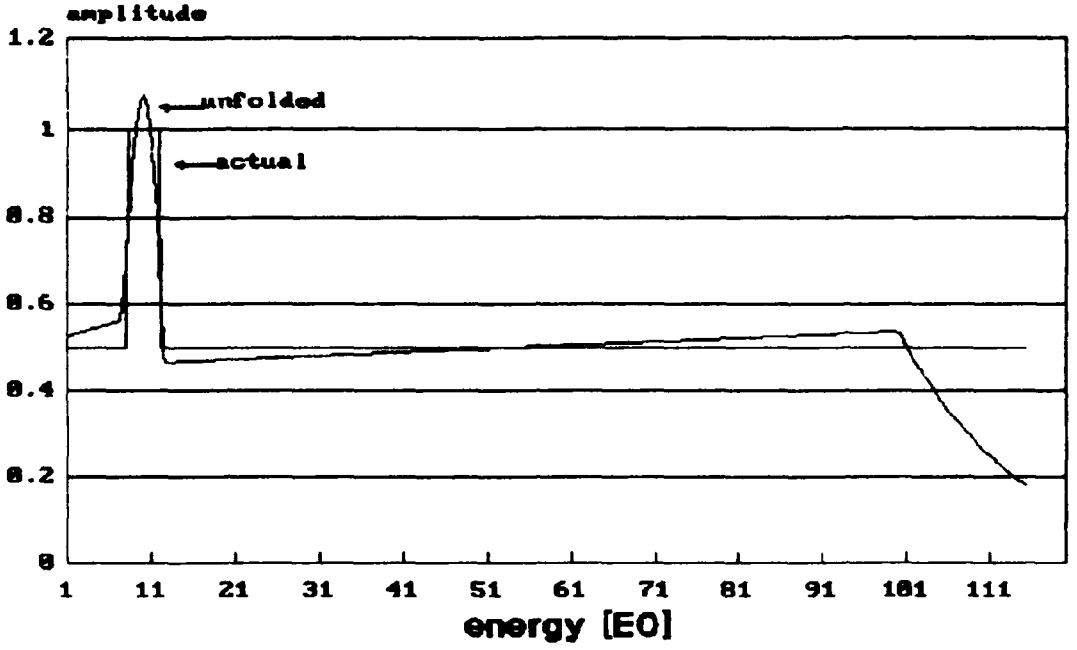

Both iteration methods, follow the triangular actual spectrum rounding off the apex and edges of the triangle similarly to the representation in case 3 as seen in figures XIX and XX. For the discontinuities studied, the iteration methods are not that particular of the shape of the spike. The cubic spline is a good representation of the actual spectrum (figure XXI), but it still has the high energy dropoff seen in the previous case.

FIGURE XIX: Modified Iteration, Test Case 4

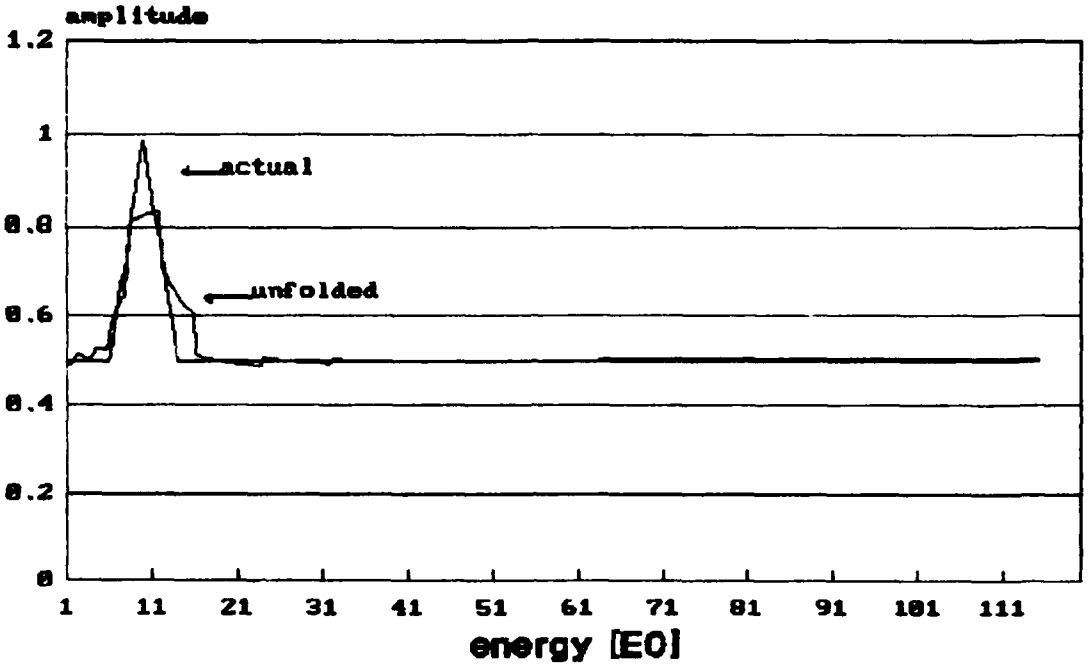

FIGURE XX: Iteration, Test Case 4

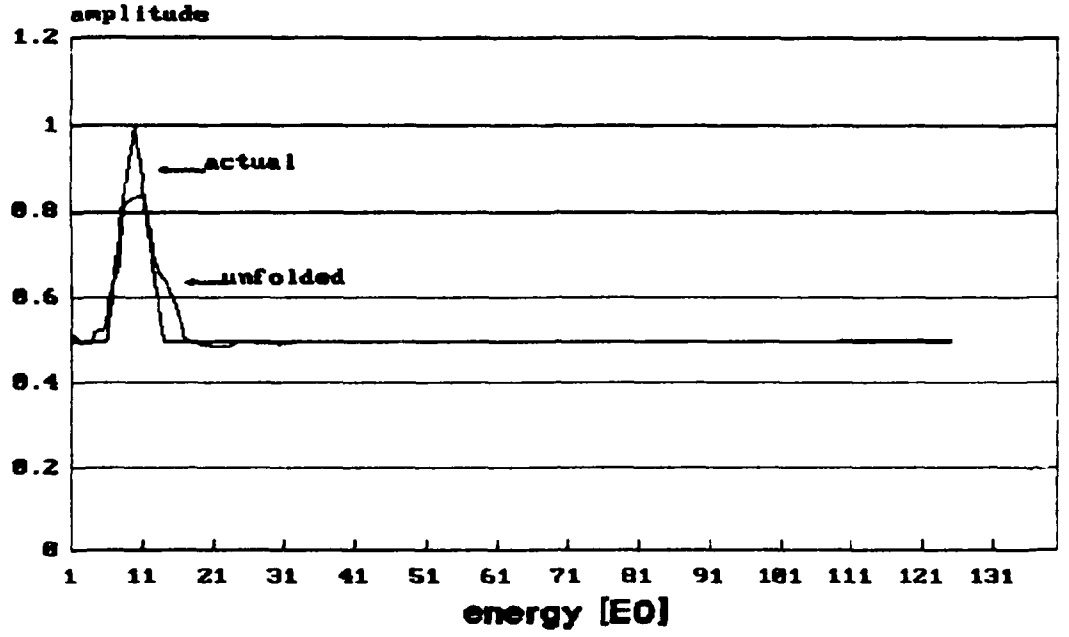

FIGURE XXI: Cubic Spline, Test Case 4

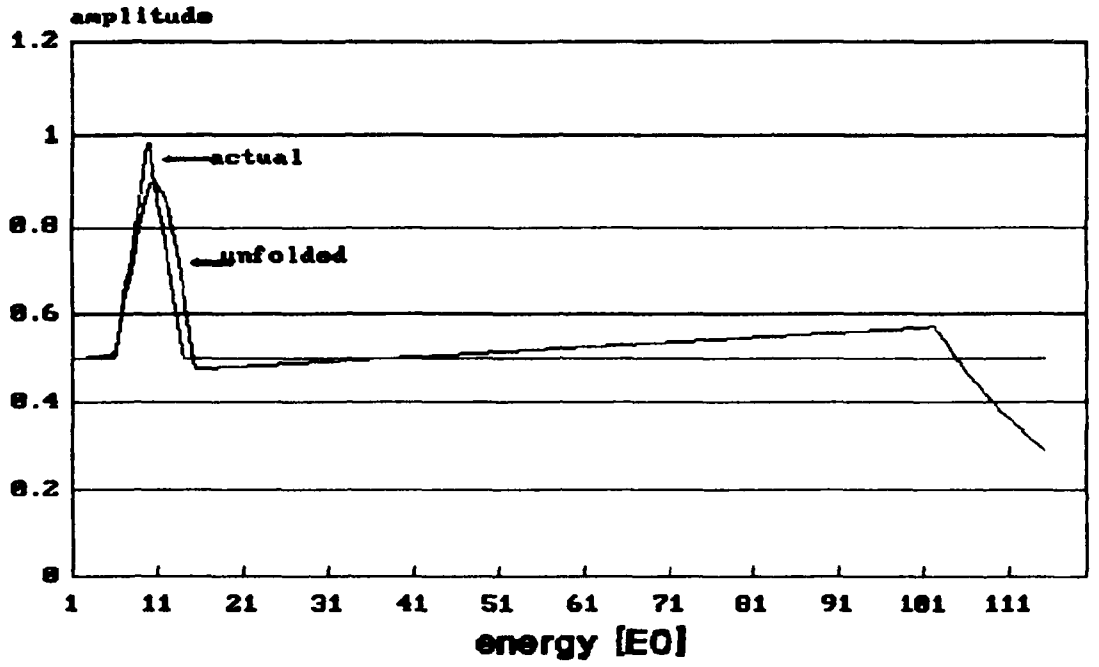

Noise on the Test Cases

For each of the test cases and unfolding methods, ten unfolded spectra were generated to determine the bars in Figures XXII and XXIII. In each of the figures the actual spectrum is graphed with the bars superimposed upon the spectrum to represent the spread of spectra due to noisy signals.

In figure XXII, the Planckian method has smaller spreads in the noisy spectra than the iteration method. But the iteration method has it's most significant spread near the pulse which the Planckian method almost ignores.

FIGURE XXII: Iteration and Planckian Unfolding Methods with Noisy Data, Test Case 1

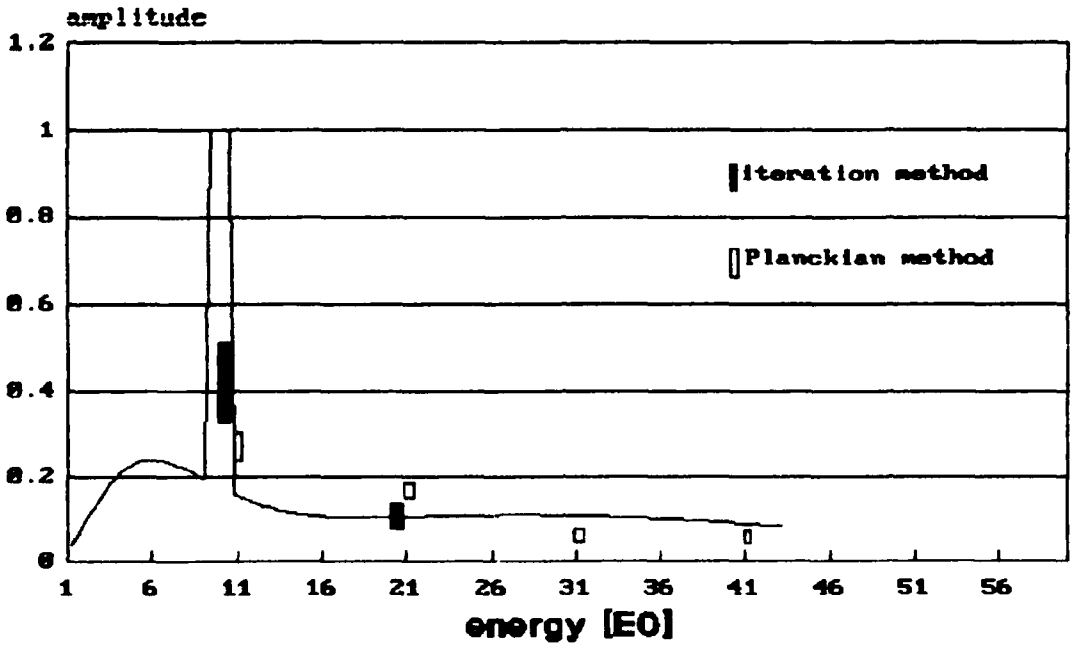

In figure XXIII, the cubic spline and iteration methods have comparable spread in their noisy spectra. Both methods have their largest spread near the spike, which both attempt to represent, and decrease with increasing energy. However the cubic spline still has large variations for large energy, where the spread of unfolded spectra from the iteration method goes to nearly zero.

FIGURE XXIII: Iteration and Cubic Spline Unfolding Methods with Noisy Data,

Test Case 4

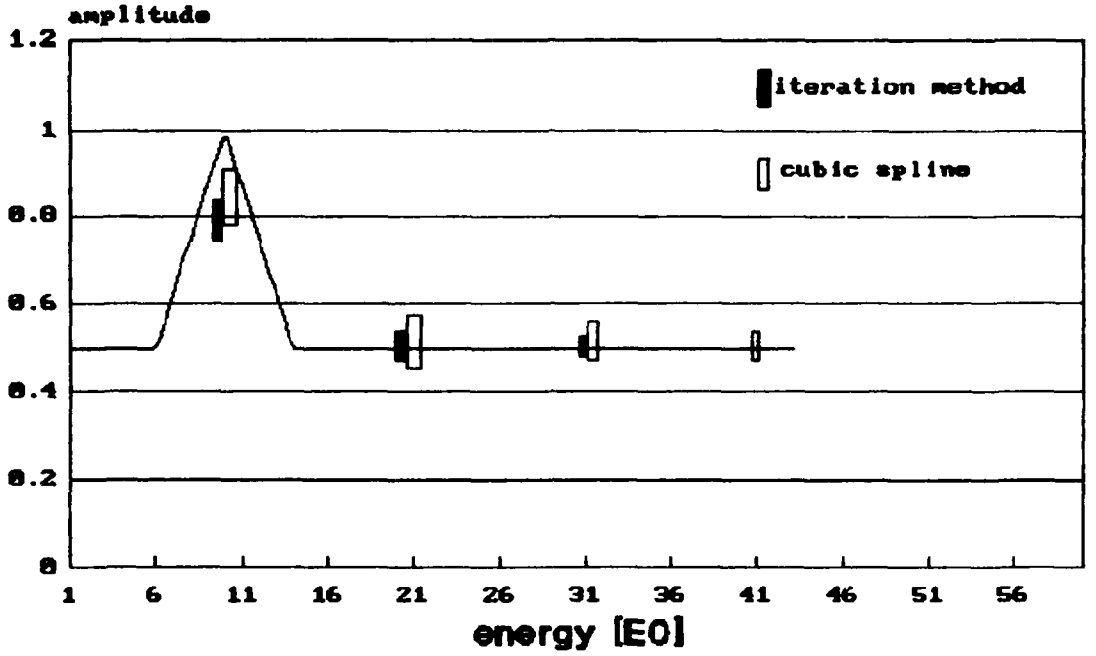

V. Summary and Conclusion

Summary

Validation of the Methods. The purpose of the validation cases is to ensure that the basis function, iteration, and the modified iteration methods were working correctly. Validation cases one through three for the basis function methods produced unfolded spectra which were nearly an exact match to the actual spectra.

The iteration and modified iteration methods produced spectra which had discontinuities near the k-edges of the response function. However the overall shape was a good representation of the actual spectra.

Test Cases. In case one, composed of two temperature Planckians and a spike, the Planckian basis method proved to be a bad representation of the actual spectrum. The method didn't indicate that the pulse was there and the overall representation was that of nearly a one temperature Planckian. The iteration methods, on the other hand proved to be more adept at approximating the shape of the spike. For case four, the iteration methods and the cubic spline were both good at representing the discontinuous shape of the spectrum. The unfolded spectrum of the cubic spline was better at representing the actual form the the spike, but it had a significant dropoff for higher energies.

The test cases for the noisy measurement signal demonstrated that the basic shape of the unfolded spectra varies considerably from trial to trial, even if there is no change in the data. The spread in the spectra is very

small for the Planckian method, but it doesn't represent the discontinuity of the spike. The spread for the cubic spline approximates that of the iteration methods for low energies, but remains large for large energies.

Conclusions:

The results from the validation and test cases indicates the following conclusion can be drawn:

1. Details of unfolded spectra, from real data produced during underground nuclears effects tests, can not be reasonably assumed to reflect real details in the actual spectra. Either the details of the actual spectra do not survive the unfolding process in the presence of noise or the details on the unfolded spectra are added during the unfolding process.
2. The actual spectrum can not be unfolded exactly, even if there were no measurement noise.
3. For actual spectra which is very nearly Planckian, the Planckian basis function method is the best. However for the test cases in this study, the iteration methods do better than the Planckian method.
4. The cubic spline method is comparable to, if not better than, the iteration method for representing discontinuous spectra. It does have significant a dropoff for higher energies and a larger spread of spectra with a noisy signal.

VI. Recommendations

The following recommendations are for continuing work in this area. First, determine the impact of more detail in the specification of the detectors e.g., different standard deviations and response functions.

Secondly, the development of another method to make the unfolded spectra more reasonable looking. Perhaps a scheme where the local points on the unfolded spectra are balanced to make the behavior of the large scale less abrupt.

Thirdly, the use of basis functions, other than Plankian and cubic splines, to represent the spectra.

Lastly, determine how the shape and size of the pulse perturbation can affect the unfolded spectrum and if there is a minimum size and shape perturbation which can be unfolded.

Bibliography

1. Abromowitz, Milton and Stegan, Irene A. (Editors). Handbook of Mathematical Functions with Formulas, Graphs, and Mathematical Tables. National Bureau of Standards, Applied Mathematics Series, 55. Washington DC: U.S. Government Printing Office, 1965.

2. Burden, Richard L. and Faires, J. Douglas. Numerical Analysis (Third Edition). Boston: PWS Publishers, 1985.

3. Daniel, Capt. Russell B. An Approximation Technique for Solving a System of Fredholm Integral Equations for Assymmetric Detector Response Functions, MS Thesis, AFIT/GNE/ENG/88M-3. School of Engineering, Air Force Institute of Technology (AU), Wright-Patterson AFB OH, March 1988.

4. Delves, L.M. and Walsh, J. (Editors), Numerical Solution of Integral Equations. Oxford, United Kingdom: Clarendon Press, 1974.

5. Gorbachenko, G.M. et al. "Use of Fluorescence in the Spectrometry of Pulsed X Radiation," Instruments and Experimental Technology, 19:244-246. Jan - Feb 1976.

6. Hewlett-Packard Company. Curve Fitting Pac Owner's Manual for the HP-71. Singapore: Hewlett-Packard Company, 1984.

7. Mathews, K.A., Air Force Institute of Technology. Private communication. (1988).

8. Selby, Samuel M. (Editor-in-Chief) "Probability and Statistics," CRC Standard Mathematical Tables (Nineteenth Edition). Cleveland, Oh: Chemical Rubber Co., 1971.

Vita

Captain Michael E. Carter [redacted] in 1973 [redacted] received a Bachelor of Science Degree in Physics from Montana State University in 1977. He was commissioned as an Air Force officer after graduating from the Officer Training School in the summer of 1980. His first assignment was at the Air Force Institute of Technology where he received his Bachelor of Science Degree in Aeronautical Engineering under the Engineer Transfer Program. He was then assigned to Headquarters Strategic Air Command (SAC) from March 1982 to July 1987. At first, he monitored the budgets of several future SAC communications systems and later compiled targeting information sent to Minuteman III intercontinental ballistic missiles. He entered the Nuclear Engineering program at the Air Force Institute of Technology in August of 1987.

[redacted]

SECURITY CLASSIFICATION OF THIS PAGE

REPORT DOCUMENTATION PAGE

Form Approved OMB No. 0704-0188

1a. REPORT SECURITY CLASSIFICATION UNCLASSIFIED	1b. RESTRICTIVE MARKINGS
2a. SECURITY CLASSIFICATION AUTHORITY	3. DISTRIBUTION/AVAILABILITY OF REPORT Approved for public release; distribution unlimited
2b. DECLASSIFICATION/DOWNGRADING SCHEDULE	
4. PERFORMING ORGANIZATION REPORT NUMBER(S) AFIT/GNE/ENG/89M-1	5. MONITORING ORGANIZATION REPORT NUMBER(S)
6a. NAME OF PERFORMING ORGANIZATION School of Engineering 6b. OFFICE SYMBOL (If applicable) AFIT/ENP	7a. NAME OF MONITORING ORGANIZATION
6c. ADDRESS (City, State, and ZIP Code) Air Force Institute of Technology Wright-Patterson AFB OH 45433-6583	7b. ADDRESS (City, State, and ZIP Code)
8a. NAME OF FUNDING/SPONSORING ORGANIZATION 8b. OFFICE SYMBOL (If applicable)	9. PROCUREMENT INSTRUMENT IDENTIFICATION NUMBER
8c. ADDRESS (City, State, and ZIP Code)	10. SOURCE OF FUNDING NUMBERS N/A PROGRAM ELEMENT NO. / PROJECT NO. / TASK NO / WORK UNIT ACCESSION NO.
11. TITLE (Include Security Classification)	
12. PERSONAL AUTHOR(S) Michael E. Carter	
13a. TYPE OF REPORT MS Thesis 13b. TIME COVERED FROM _____ TO _____	14. DATE OF REPORT (Year, Month, Day) 1989 March 15. PAGE COUNT 68
16. SUPPLEMENTARY NOTATION	

17. COSATI CODES			18. SUBJECT TERMS (Continue on reverse if necessary and identify by block number)
FIELD	GROUP	SUB-GROUP	Fredholm Integral Equations X-ray Diagnostics
18	4		

19. ABSTRACT (Continue on reverse if necessary and identify by block number)

Title : Comparison of Iteration and Basis Function Methods for Solving the Fredholm Integral Equation of the First Kind

Thesis Chairman: Kirk A. Mathews, LCDR, USN
Associate Professor of Nuclear Engineering (Effects)

20. DISTRIBUTION/AVAILABILITY OF ABSTRACT ☒ UNCLASSIFIED/UNLIMITED ☐ SAME AS RPT. ☐ DTIC USERS	21. ABSTRACT SECURITY CLASSIFICATION UNCLASSIFIED
22a. NAME OF RESPONSIBLE INDIVIDUAL Kirk A. Mathews, LCDR, USN	22b. TELEPHONE (Include Area Code) (513) 255-3030 22c. OFFICE SYMBOL AFIT/ENG

DD Form 1473, JUN 86 *Previous editions are obsolete.* SECURITY CLASSIFICATION OF THIS PAGE

UNCLASSIFIED

Abstract

The purpose of this study is to compare methods for solving the Fredholm integral equation of the first kind. The Fredholm equation has several practical applications including geology, superconductivity, and aerodynamics. Of specific interest is its application to determining radiation spectra using data from underground nuclear effects simulations.

The two basic methods studied were the basis function method and the iteration method. The basis function method is a representation of the unfolded spectrum by a series of Planckian or cubic spline functions. The iteration method scales the unfolded spectrum so that its weighted integral over a given interval matches that of the actual spectrum.

Both the basis function methods produced excellent results when the actual spectrum was a sum of it's basis functions. The cubic spline method produced unfolded spectra which were good approximations for discontinuous actual spectra. However, there was a significant dropoff of the spectrum for the cubic spline unfolded spectra for higher energies.

The iteration methods produced accurate approximations for actual spectra that were both basis functions and/or discontinuous spectra. There were two problems with this method: the iteration method produced spectra which were discontinuous at the discontinuities of the weighting function and noisy data can produce large discontinuities in the unfolded spectrum.

For the cases studied, the iteration method is the best method, because of it's ability to unfold a variety of spectra (in contrast to the Planckian basis function method) and it's good behavior at the higher energies for noisy data (in contrast to the cubic spline method).